THE JOURNAL OF PHYSICAL CHEMISTRY A

Article

pubs.acs.org/JPCA

High-Resolution Direct-Absorption Spectroscopy of Hydroxymethyl Radical in the CH Symmetric Stretching Region

Melanie A. Roberts, Erin N. Sharp-Williams, and David J. Nesbitt*

JILA, University of Colorado, National Institute of Standards and Technology, and Department of Chemistry and Biochemistry, University of Colorado, Boulder, Colorado 80309, United States

ABSTRACT: High-resolution, fully rotationally resolved direct absorption spectra of hydroxymethyl radical, CH_2OH, are presented in the infrared CH stretching region. As a result of low rotational temperatures and sub-Doppler linewidths obtained in the slit supersonic expansion, the $K_a = 0 \leftarrow 0$ band of the symmetric CH stretch for CH_2OH has been unambiguously identified and analyzed. By way of chemical confirmation, hydroxymethyl radical is generated via two different slit jet discharge syntheses: (i) direct dissociation of CH_3OH to form CH_2OH and (ii) dissociation of Cl_2 followed by the radical H atom extraction reaction $Cl + CH_3OH \rightarrow HCl + CH_2OH$. The identified transitions are fit to a Watson A-reduced symmetric top Hamiltonian to yield first precision experimental values for the ground state rotational constants as well as improved values for the symmetric stretch rotational constants and vibrational band origin. The results both complement and substantially improve upon spectral efforts via previous double resonance ionization detected infrared methods by Feng et al. [*J. Phys. Chem. A*, **2004**, *108*, 7093], as well as offer high-resolution predictions for laboratory and astronomical detection of hydroxymethyl radical in the millimeter-wave region.

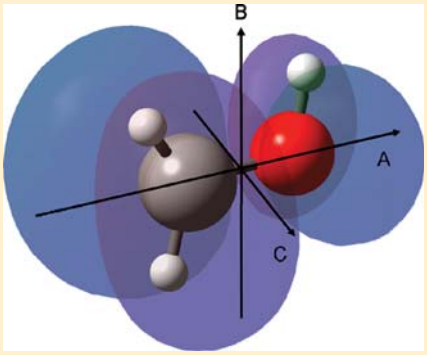

I. INTRODUCTION

Hydroxymethyl radical, CH_2OH, has been the subject of over 100 experimental and theoretical papers in the last 40 years,[1] in large measure due to the important role it plays as a reactive intermediate in combustion and environmental chemistry.[2] As one example, the combustion initiation step for oxygenated hydrocarbon fuels such as methanol is thought to be hydrogen abstraction by O_2 to produce hydroxymethyl radical, i.e., $CH_3OH + O_2 \rightarrow CH_2OH + HO_2$.[3,4] There is also central involvement of hydroxymethyl radical in many of the subsequent chain reaction kinetics, for example, a fundamental chain propagation step in the oxidative combustion of methanol is $CH_3OH + HO_2 \rightarrow CH_2OH + H_2O_2$. Indeed, real time monitoring capabilities for CH_2OH radical in methanol combustion, as well as a detailed understanding of the underlying kinetics would be very desirable in optimizing combustion processes.[4−7] Significantly complicating this task is the ubiquitous presence of methoxy radical (CH_3O) in many combustion systems, which has the same chemical composition as hydroxymethyl radical. This makes mass spectrometry a less versatile method for monitoring the underlying radical kinetics, although the recent combination of synchrotron VUV photoionization and mass spectroscopy looks to be especially promising.[8−13]

In addition to fundamental combustion processes, hydroxymethyl radical is an important intermediate for oxidative reactions occurring in the troposphere. Indeed, atmospheric scrubbing reactions of alkanes, alkenes, and alcohols all involve hydroxymethyl radical as a reactive intermediate.[3,5,14−17] Alkenes account for about 10% of the nonmethane organic compound concentration in many urban areas as a result of gasoline-based fuels and motor vehicle exhaust emissions.[18] The initial oxidative scrubbing reactions of simple alkenes such as ethene are initiated by hydroxyl (OH) radical attack,[19] which features several steps involving CH_2OH as an intermediate.[17,18] Furthermore, methanol itself has a nontrivial concentration in the troposphere,[20] ranging from 400 to 700 ppt depending upon the latitude, with about 85% of atmospheric oxidative scrubbing reactions producing hydroxymethyl radical as a transient intermediate.[18]

As a third area of relevance and interest, hydroxymethyl radical is likely to be an abundant polyatomic hydrocarbon species in the interstellar medium.[21−24] Indeed, the precursor methanol molecule is ubiquitous in interstellar spectroscopic observations, so much so that it is considered a challenging source of background transitions in the millimeter (mm)-wave and/or far-infrared (IR) spectrum.[25−31] In the presence of abundant high energy VUV light in the interstellar regions, the photodissociation lifetime of methanol to form hydroxymethyl radical is expected to be rather short.[21,22] This suggests the possibility of direct detection of CH_2OH by far-IR and/or mm-wave (or possibly even near IR-) spectroscopy, which, in conjunction with spectrally measured methanol densities, could provide interesting information on high energy radiation flux levels involved in photofragmentation.[23,24] Alternatively and of particular relevance to the present work, high-resolution

Special Issue: Joel M. Bowman Festschrift

Received: December 31, 2012
Revised: January 25, 2013
Published: January 28, 2013

   dx.doi.org/10.1021/jp312877k | *J. Phys. Chem. A* 2013, 117, 7042−7049

observation and assignment of CH_2OH spectral transitions in the near-IR could greatly facilitate spectral search and detection via lab-based studies in the far-IR/submm-wave region.[32,33] This, in turn, could significantly advance future prospects for successful search for these species in the interstellar medium with new far-IR/submm telescope capabilities coming on line.[34−36]

The above examples provide strong motivation for development of high-resolution near-IR experimental tools for spectroscopic identification of hydroxymethyl radical, as a key reactive intermediate in combustion, atmospheric, and interstellar chemical reactions. Such keen levels of interest have spurred significant spectroscopic efforts. The earliest such studies on hydroxymethyl radical were based on electron spin resonance (ESR) detection, which, in conjunction with high level ab initio theoretical efforts, predicted a quasi-planar structure of the radical.[37−41] Low-resolution infrared detection of CH_2OH radical was first obtained by Jacox via matrix isolation spectroscopy and UV photolysis of methanol, which identified several vibrational modes in the fingerprint region.[42,43] These pioneering efforts, in turn, stimulated a plethora of additional theoretical, spectroscopic, and kinetic studies.[2,19,33,44−46] Of particular relevance to our work is a series of resonance enhanced multiphotoionization (REMPI) studies by Hudgens and co-workers, which identified multiple Rydberg states and Franck−Condon active vibrational progressions in these lower and upper state manifolds.[47−49]

In order to facilitate interpretation of their spectral data, Hudgens and co-workers calculated a 2-dimensional potential energy surface at the MP2/6-311G(2df,2p) level for the lowest frequency OH torsion (ν_8) and CH_2 (ν_9) wag coordinates, yielding detailed energy/frequency predictions for these two coupled modes.[1,47,48] By way of example, their potential surface calculations predict the frequency of the first excited ν_9 wag mode at 238 cm^{-1}, which is in excellent agreement with the observed value at 234 ± 5 cm^{-1}. Furthermore, these studies determined that quantum state labels for these two modes remained approximately separable, at least for vibrational energies sufficiently low with respect to the (~1700 cm^{-1}) OH torsional barrier height. Most importantly, the presence of such a torsional barrier predicts closely spaced tunneling levels, specifically with splittings between ground and first excited torsional modes (ν_8) lower than the ~1 cm^{-1} precision of the calculations.[1] On the basis of such an upper limit for these torsional splittings, one expects both ground and first excited tunneling levels to be populated even under jet-cooled conditions (T_{rot} = 20−30 K), and thus the possibility for line doubling in high-resolution near-IR spectra.

More recently, Reisler and co-workers have performed a number of studies on dissociation dynamics and the spectroscopy of hydroxymethyl radical.[2,50−56] In particular, these studies elucidated the spectroscopy of low lying electronic states including the 3s, $3p_x$, and $3p_z$ Rydberg levels as well as the CH symmetric stretch, CH asymmetric stretch, and OH stretch fundamental and first overtone. Specifically, Feng et al. exploited double resonance ionization detected IR spectroscopy via the $3p_z$ Rydberg state to probe both CH and OH stretch spectral regions with ~0.4 cm^{-1} laser line width and thus achieving partial rotational resolution. Least squares analysis of the rovibrational band contours yielded (i) vibrational band origins and (ii) A, B, and C rotational constants for the upper states, based on ab initio estimates for the ground state. The antisymmetric CH stretch and OH stretch spectra closely matched theoretical predictions of pure B-type and mixed A/B-type bands, respectively, as predicted by ab initio calculations. In contrast, the symmetric CH stretch was theoretically predicted to be predominantly A-type but in fact required a more mixed 60% A-type/40% B-type character to adequately fit the data. Furthermore, Feng et al. did not see any evidence of additional doubling structure in their spectral data due to tunneling across the OH torsional barrier, which provided a 10-fold lower estimate (< 0.1 cm^{-1}) for any putative tunneling splittings in the ground state.

In this current study, we have built on the pioneering work of Reisler and co-workers to help guide a near IR search for hydroxymethyl radical with sub-Doppler, fully rovibrationally resolved spectral resolution. Figure 1 shows the equilibrium structure and principle axes of hydroxymethyl radical, obtained via CCSD(T)/AVQZ calculations in MOLPRO.[57] Although we have very good estimates from the previous studies for all three H-stretching bands, we have chosen first to focus on the symmetric CH stretch spectral region near 3043 cm^{-1}, which is predicted to have the highest integrated CH band intensity. Indeed, we observe a surprisingly rich spectrum in this region, partially congested by discharge induced hot band transitions in methanol, which is still under further analysis. However, as the first high-resolution data on this critical combustion radical, we have been able to unambiguously identify and assign the K_a = 0 ← 0 progression of symmetric stretch excited CH_2OH, which serves as the primary focus of this article.

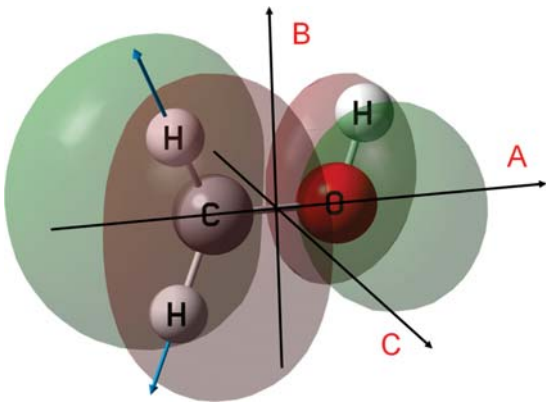

Figure 1. Quasi-planar structure of hydroxymethyl radical with HOMO, predominant OH stretch normal mode coordinate, and principle axis orientation shown. Though small enough not to be immediately evident, the equilibrium geometry has a slightly bent methyl group in the out-of-plane bend coordinate, due to competition between sp^3 and sp^2 hybridization around the central C atom.

II. EXPERIMENTAL SECTION

The high-resolution infrared spectrometer used in these experiments has been described in detail elsewhere and can be briefly summarized.[58−60] Narrow-line width (<2 MHz), high-precision infrared light is generated by difference frequency generation of a single frequency argon ion laser (Ar^+) and a tunable cw dye laser (R6G, Exciton dyes) in a temperature tuned periodically poled lithium niobate ($LiNbO_3$) crystal. The infrared radiation is split into reference and signal beams, with the reference beam directed onto a liquid-nitrogen cooled InSb detector. The signal beam enters a 16-multipass Herriot cell in the slit jet discharge expansion vacuum chamber

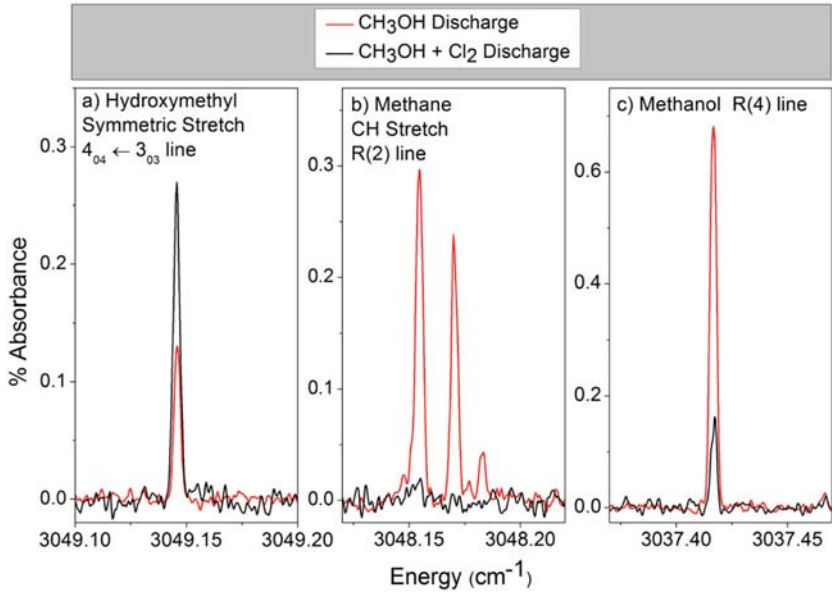

Figure 2. Comparison of two different discharge chemistries for the synthesis of jet-cooled CH_2OH. The red line represents three sample high-resolution spectral regions for a discharge with CH_3OH doped into Ne70 diluent. The corresponding black line illustrates comparable data scans for a $CH_3OH + Cl_2$ discharge, which generates hydroxymethyl radical via $Cl + CH_3OH \rightarrow HCl + CH_2OH$ chemistry. Panel a reveals how CH_2OH radical density approximately doubles for chemical formation via H atom abstraction by discharge generated Cl atoms. Interestingly, panels b and c also reveal how the spectral density of undesired species (such as methane and precursor methanol) can be substantially minimized via the Cl atom reactive synthesis pathway.

through a CaF_2 window, with each pass sampling a 4 cm long path length of jet cooled radicals. Spectra of CH_2OH radical are recorded via transient depletion of the transmitted IR light monitored by the signal InSb detector. The signals from the two detectors are combined in a common mode noise subtractor before being sent to a lock-in detector and subsequently recorded on a computer (via a NI-6025E analogue-digital card). Relative frequency precision (10 MHz) is obtained by monitoring dye laser fringes through an actively stabilized (<1 MHz rms) Fabry–Perot etalon, with the Ar^+ laser actively locked to the same Fabry–Perot cavity to provide single frequency operation and stability while scanning. Absolute frequency calibration is achieved by comparison with well characterized ν_3 CH stretch absorptions of jet cooled methane doped into the expansion and monitored in the same spectral region.[61]

Jet-cooled hydroxymethyl radicals are produced by supersonic expansion of trace amounts of precursor in 70% neon, 30% helium (Ne70) buffer gas mixture through a pulsed slit jet nozzle (19 Hz, 500 μs duration). Radicals are generated via electron associative detachment in a square-wave modulated (50 kHz) discharge at the expansion orifice. For the many radicals previously studied with this apparatus, the precursor has been designed to contain a weak bond cleavage point (e.g., C–Br or C–I) to form the desired target radical, typically by dissociative attachment. Such precursors for hydroxymethyl are unstable, which led us to develop two recipes based on methanol, though this requires cleavage of a strong CH bond. Our first approach, i.e., simply a Ne70 discharge with trace methanol, is successful in generating quite good concentrations of hydroxymethyl radical but also generates spectral interferences from methane and vibrationally excited methanol. Our second approach is based on doping Cl_2 into the Ne70/methanol discharge expansion, which generates hydroxymethyl by more selective CH bond abstraction reactions of $Cl + CH_3OH \rightarrow CH_2OH + HCl$ and, most importantly, yielding fewer spectral interferences.[62−64]

Figure 2 shows sample spectral data generated with the two different synthesis approaches: (i) CH_3OH in Ne70 discharge (red) and (ii) $CH_3OH + Cl_2$ + Ne70 discharge (black). The first panel plots the CH_2OH $4_{04} \leftarrow 3_{03}$ ($N'_{Ka' Kc'} \leftarrow N''_{Ka'' Kc''}$ labeling) line, which shows an approximate 2-fold increase in absorbance upon the addition of Cl_2 (spectral assignments to be discussed in section III). The second panel illustrates that a methanol discharge yields methane, but essentially vanishes for a Cl_2-doped discharge. The third panel represents a sample methanol absorption line that illustrates a desirable decrease in precursor absorption with the addition of Cl_2 molecular chlorine. While both sources of CH_2OH radical yield spectra relatively congested in the symmetric CH stretch region, the synthesis with Cl_2 clearly represents the pathway with reduced spectral interferences.

III. RESULTS AND ANALYSIS

A sample R-branch region of the CH_2OH symmetric stretch band is shown in Figure 3, with representative experimental data and assignments plotted (panel a), a Watson asymmetric top Hamiltonian (A-reduction) simulation (panel b) based upon least-squares fit to the data (see below), and an inset of the $1_{01} \leftarrow 0_{00}$ transition (panel c) highlighting the respectably high (>10:1) signal-to-noise. These hydroxymethyl radical lines represent the lowest three R-branch lines in the $K_a = 0 \leftarrow 0$ progression, which will be the highest intensity progression based upon ortho/para nuclear spin statistics, as discussed below. Guided by Reisler and co-workers predictions for the symmetric stretch rotational constants and band origin, we are able to identify a full P branch ($3_{03} \leftarrow 4_{04}$) to R branch ($7_{07} \leftarrow 6_{06}$) progression of A-type $K_a = 0 \leftarrow 0$ lines, with an approximate (B + C) $\approx$ 1.86 cm^{-1} spacing. By way of additional

dx.doi.org/10.1021/jp312877k | J. Phys. Chem. A 2013, 117, 7042–7049

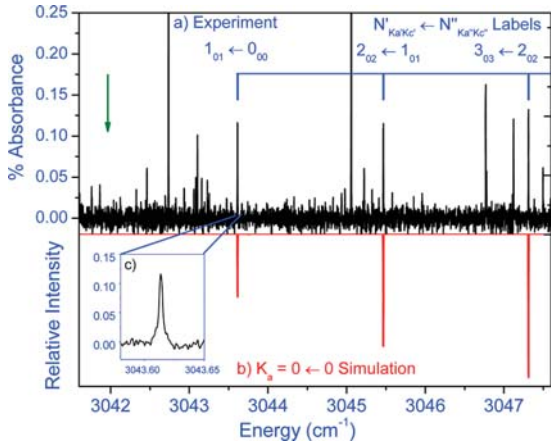

Figure 3. Sample data shown with simulation based upon least-squares fits to a Watson asymmetric top Hamiltonian. Panel a reveals a spectral scan region near the ν_3 symmetric CH stretch band origin, with assignment of the $K_a = 0 \leftarrow 0$ progression shown above (in blue). The green arrow indicates the missing line in the progression that makes the band origin assignment and *J*-labeling unambiguous. Panel b provides a spectral simulation (in red) of the A-type band $K_a = 0 \leftarrow 0$ progression based upon spectroscopic constants from the least-squares fit. The blow up region in panel c illustrates a single $1_{01} \leftarrow 0_{00}$ absorption line in the ν_3 band, which serves to characterize typical signal-to-noise levels of >10:1 in the current experiment.

confirmation, we also compare the spectral data obtained with two different chemical mechanisms of generating hydroxymethyl radical, as described above. While the same $K_a = 0 \leftarrow 0$ lines progression appears with both source chemistries, the signals are approximately twice as intense when formed by Cl radical abstraction from methanol. Indeed, this closely mirrors the efforts by Reisler and co-workers, who report efficient production of CH_2OH radical in a supersonic jet by UV photolysis of Cl_2 followed by H atom abstraction.[2,53,55,56]

The absence of Q-branch lines for an A-type $K_a = 0 \leftarrow 0$ band greatly facilitates high-resolution identification of the spectral band origin. Specifically, the spectrum indicates an approximately 2-fold larger spacing (i.e., ~2(B + C)) between the lowest R branch $1_{01} \leftarrow 0_{00}$ and P-branch $0_{00} \leftarrow 1_{01}$ lines, which unambiguously identifies the band origin to be at 3041.7560(5). We note that this differs from the study of Feng et al.,[55] where the band origin is obtained from fits to the rotational band contours and is reported to be 3043.3 cm^{-1}. However, one obvious advantage of the present study is a ~100-fold increase in spectral resolution, which makes identification of this missing $K_a = 0 \leftarrow 0$ Q-branch region immediately apparent. Given that there is clearly rotational structure in the study by Feng et al., it seems likely that such differences in the two spectral analyses arise simply from a $\Delta J = 2$ registry shift in the *J* assignment, as correctly summarized in Table 1.

The key motivation for the present work has been to provide precision predictions with which to facilitate spectral search efforts in other laboratories for CH_2OH radical in the far-IR/mm-wave region. Because of the finite information content in a single $K_a = 0 \leftarrow 0$ progression, we are restricted in the level of Hamiltonian modeling used in the least-squares fitting procedure. However, the precision of the spectral data and molecular asymmetry of the radical is sufficiently large to independently determine B and C rotational constants in both the upper and lower vibrational states. Specifically, we least-

Table 1. Experimental Line Positions of the $K_a = 0 \leftarrow 0$ Progression with Assignments Using the $N'_{Ka' Kc'} \leftarrow N''_{Ka'' Kc''}$ Notation; Obs − Calcd Values Are Based on Predictions from the Least Squares Fitted Rovibrational Constants Reported in Table 2

$N'_{Ka' Kc'}$	$N''_{Ka'' Kc''}$	experimental frequency (cm^{-1})	obs − calcd ($\times 10^{-4}$ cm^{-1})
3_{03}	4_{04}	3034.3183	1
2_{02}	3_{03}	3036.1742	−2
1_{01}	2_{02}	3038.0342	0
0_{00}	1_{01}	3039.8959	3
1_{01}	0_{00}	3043.6137	−3
2_{02}	1_{01}	3045.4665	0
3_{03}	2_{02}	3047.3112	0
4_{04}	3_{03}	3049.1460	2
5_{05}	4_{04}	3050.9677	−1
6_{06}	5_{05}	3052.7747	−1
7_{07}	6_{06}	3054.5650	1

squares fit the $K_a = 0 \leftarrow 0$ progression to a Watson A-reduction asymmetric top Hamiltonian, with the A rotational constants fixed at ab initio values (A″ = A′ = 6.450 cm^{-1}) obtained from our highest level MOLPRO calculations at the CCSD(T)/AVQZ level of the CH_2OH potential minimum.[57]

The fit results are summarized in Table 2, with simulated spectral predictions based upon these constants shown in panel

Table 2. Comparison of Molecular Constants (in cm^{-1}), Based on Least Squares Fit to a Watson A-Reduced Asymmetric Top Hamiltonian Model (With Fixed at ab Initio Values A′ = A″ = 6.45 cm^{-1}); the Number in Parentheses Represents the Error on the Last Digit

	ab initio values	previous work[55]	present work[c]
B″	0.9984[a]		0.9951(6)
C″	0.8722[a]		0.8656(5)
B′		0.93	0.9945(4)
C′		0.88	0.8632(3)
ν_3	3022(10)[b]	3043.3	3041.7563(1)

[a]MOLPRO ab initio calculations at the CCSD(T)/AVQZ level.[57] [b]Estimates from calculations at the B3LYP\6-311++g(3df,3pd) level,[72] with a harmonic band origin scale factor of 0.9637 based on Dong et al.[60] [c]Residual standard deviation σ = 0.00024 cm^{-1} (7.2 MHz).

b of Figure 3 and observed minus calculated values in Table 1. Even with this simplified Hamiltonian, the quality of the spectral fit is extremely good, with residual standard deviations (0.00024 cm^{-1} = 7.2 MHz) already smaller than our typical experimental frequency accuracy estimates of <10 MHz. Though there are sizable differences between the present fitted B′ and C′ rotational constants and previously reported values (+7.0% and −1.6%, respectively), the ground state results are now in much better agreement with our highest level MOLPRO predictions (CCSD(T)/AVQZ), with the anticipated slight *decrease* in B and C (−0.33% and −0.71%) due to anharmonic zero point quantum motion of the CH bond. Indeed, this improved agreement is echoed between the lower and upper state B and C rotational constants, with a small but significant decrease ($\Delta B \approx -0.06\%$ and $\Delta C \approx -0.27\%$) consistent with extension of the CH bond length due to symmetric stretch excitation. Indeed, as a final consistency test, the molecular asymmetry predicted from the fitted B and C rotational constants is also in good agreement with the ab initio

dx.doi.org/10.1021/jp312877k | J. Phys. Chem. A 2013, 117, 7042−7049

A value (i.e., $(1/C - 1/B)^{-1} \approx 6.65$ cm^{-1} vs 6.45 cm^{-1}) predicted for a near planar CH_2OH radical geometry with a nearly zero inertial defect.

IV. DISCUSSION

In spite of spectral congestion and limited line assignment, the current data provides useful diagnostics with which to characterize the discharge chemistry as well as rotational temperature in the slit-jet expansion. The intensity of any one rovibrational line reflects a product of lower state population, intrinsic vibrational band strength, Hönl-London factor, $2J + 1$ degeneracy, and a Boltzmann factor of lower state energy and jet rotational temperature. Figure 4 presents a standard semilogarithmic Boltzmann plot of the experimental populations vs rotational energy of the lower state, with black circles (red sqaures) representing (i) $CH_3OH + Cl_2$ discharge synthesis vs (ii) CH_3OH only discharge. The fit quality indicates rotational populations of both synthesis are reasonably well described by a single rotational temperature that does not differ within least-squares fitting uncertainty between the two syntheses (T_{rot} = 30(6) K and 28(3) K, respectively). However, the difference between the two intercepts does differ significantly and demonstrates a 2.3-fold greater efficiency for CH_2OH formation upon the addition of Cl_2 to the discharge.

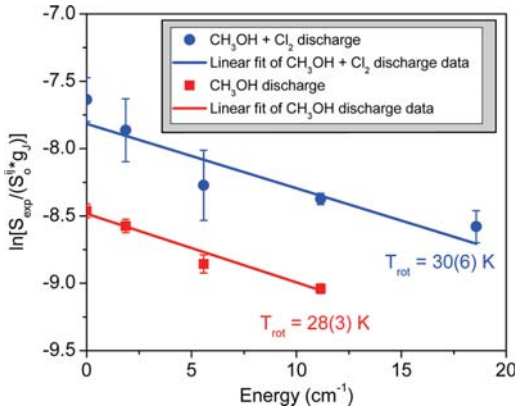

Figure 4. Boltzmann analysis of ν_3 symmetric CH stretch band spectral line intensities for jet-cooled CH_2OH radical obtained under both (i) CH_3OH doped discharge (red squares) and (ii) Cl_2/CH_3OH discharge (blue circles) conditions. S_{exp} is the integrated line strength in units of absolute absorbance), with S_{ij} and $g_J = 2J + 1$ representing the line strength factor and m_J degeneracy, respectively. The lower signal levels in the CH_3OH vs Cl_2/CH_3OH discharges reflect lower densities of CH_2OH radical. Comparison of logarithmic intercepts indicates an approximately 2-fold greater efficiency for CH_2OH radical generation under Cl_2/CH_3OH-doped discharge conditions.

The quantum state resolved populations of CH_2OH in the jet expansion are also influenced quite generally by nuclear spin statistics due to equivalence of the methylenic hydrogen atoms for any finite height barrier.[65] More specifically, this exchange symmetry arises by combination of (i) COH torsional motion over (even) a high barrier and (ii) CH_2 wagging motion over a low barrier, which is formally equivalent to a C_2 rotation of the (C_{2v}) planar tunneling transition state around the A axis. Interchange of the hydroxyl H with methylenic H atoms may occur but is likely infeasible on resolution limited experimental time scales (<10 MHz; >16 ns) and therefore need not be considered. Referenced to the planar C_{2v} transition state, Fermi−Dirac statistics for the identical methylenic H atoms ($I_H = 1/2$) require the total wave function $\Psi_{tot} = \Psi_{elec}\Psi_{tor}\Psi_{vib}\Psi_{rot}\Psi_{nuc\ spin}$ to be antisymmetric with respect to C_2 rotation. The electronic wavefuntion Ψ_{elec} for such a π radical (see Figure 1) is antisymmetric with respect to C_2 operation, with the torsion-vibrational wave function ($\Psi_{tor}\Psi_{vib}$) symmetric for the vibrationless ground state. However, the rotational wave function (Ψ_{rot}) is symmetric (antisymmetric) for K_a = even (odd) at the C_{2v} transition state, which therefore predicts a 3:1 nuclear spin statistic ratio for $K_a = 0/K_a = 1$ states, respectively. Conversely, the first excited tunneling level is *antisymmetric* in Ψ_{tor}, therefore yielding $K_a = 0/K_a = 1$ states with *inverted* 1:3 nuclear spin statistics. Overall, this implies the absence of any nuclear spin statistical alternation with J state for a given K and tunneling subband (as indeed confirmed in Figure 3) and predicts a 3-fold *decrease* in the total line intensity for the $K_a = 1 \leftarrow 1$subband.[65]

Though the present work represents first fully rovibrationally resolved IR spectroscopic data for CH_2OH radical, much more analysis remains to be done. One obvious question is why the corresponding $K_a = 1 \leftarrow 1$ progression is not readily assigned in this same spectral region spectrum. Though nuclear spin statistics will reduce the $K_a = 1/K_a = 0$ signal ratio by an additional 3-fold, our current $K_a = 0 \leftarrow 0$ signal intensities suggest that the corresponding $K_a = 1 \leftarrow 1$ subband should be readily visible above noise levels. One dynamically interesting possibility is that large amplitude quantum motion in the CH_2 wagging coordinate leads to a strong vibrational and torsional state dependence to the effective A constant, resulting in significant K_a dependent shifts in the $\Delta K_a = 0$ subband origins. We have made some progress in this direction by solving for eigenvalues and eigenfunctions on the ab initio 2D COH torsional/CH_2 wagging potential energy surface obtained at the CCSD(T)/AVQZ level. However, this would also be an ideal target for vibrational MULTIMODE calculations on permutationally invariant potential surfaces in higher (ideally, full $3N - 6 = 9$) degrees of freedom, such as developed so successfully by Bowman and co-workers.[30,31,66,67]

A second issue is why we do not see a similar progression for the asymmetric tunneling state arising from COH torsional excitation, which is thought to be <1 cm^{-1} above the ground state and would therefore clearly be thermally populated under 30 K supersonic slit expansion conditions. One important consideration is that selection rules in such torsional hot bands correspond to upper ← upper and lower ← lower tunneling level transitions.[65] As a result, these band origins will be shifted by the *difference* in tunneling splitting between the ground and excited symmetric CH stretch state. If the tunneling splittings in both states were < 1 cm^{-1}, one would therefore expect from nuclear spin statistics a $K_a = 1 \leftarrow 1$ progression corresponding to upper ← upper tunneling transitions of comparable strength to the $K_a = 0 \leftarrow 0$ lower ← lower progressions reported herein. Further scanning, identification and assignment of these progressions in both the ground and excited tunneling states clearly represent critical directions for ongoing efforts.

A third issue worth noting is that we do not see any B-type progressions out of the CH_2 symmetric stretch. Indeed, any appreciable B-type component to the reported A-type band of this near prolate asymmetric top should be particularly visible due to the strong Q-branch transitions predicted near the band origin. Given current signal-to-noise on the A-type band, we estimate any B-type band strength to be <10%. This differs

from predictions from previous least-squares fits to CH_2OH spectral band contours, which suggest a 40%/60% B-type/A-type ratio of band strengths. Interestingly, a <10% B-type/A-type band strength ratio would be in fact consistent with ab initio calculations, which predict a dipole derivative dominated by motion along the A-axis and therefore a much smaller B-type transition moment. However, further scanning and assignment efforts will be necessary to make a more quantitative comparison.

As a final comment and tribute, we note that these relatively small but highly reactive combustion radicals such as CH_2OH offer a profound and enduring challenge to the state-of-the art in both ab initio quantum mechanics and theoretical dynamics, a direction in which Professor Bowman has been a pioneer and leader for many decades.[2,66−71] His elegant work in generating both (i) high-quality permutationally invariant potential surfaces for small polyatomic closed shell and radical species[67,69−71] and (ii) full multidimensional quantum calculations[30,31,66] of the nuclear dynamics on these surfaces has established a remarkably high bar for rigor, as well as close interaction and collaboration between detailed theory and experiment. We would like to take this opportunity to thank Professor Bowman for his many pioneering contributions to the field of dynamics of highly reactive molecules. Indeed, we hope that the present work on hydroxymethyl radical provides yet one small example of how high-resolution direct infrared absorption spectroscopy on transient species cooled to low temperatures may continue to provide future challenges for the Bowman group to tackle!

V. CONCLUSIONS AND SUMMARY

First, fully rotationally resolved high-resolution spectra of hydroxymethyl radical have been obtained in the $K_a = 0 \leftarrow 0$ symmetric CH stretch region, resulting in much improved experimental values for ground state rotational constants and vibrational band origin. Additional confirmation of the spectra arising from hydroxymethyl radical is achieved by synthesizing the radical in two different ways: (i) electron bombardment cleavage of methanol doped in a supersonic discharge expansion ($CH_3OH \rightarrow CH_2OH + H$) and (ii) selective chemical H atom removal by $Cl + CH_3OH \rightarrow CH_2OH + HCl$ reactions in a Cl_2 and methanol doped discharge. The precision of the ground state rotational constants provide high quality frequency predictions with which to minimize spectral search and thereby enable further laboratory detection and characterization of this highly reactive radical in the microwave, mm-wave, far-IR, and near-IR spectroscopic regions. The large amplitude COH torsional tunneling and out of plane CH_2 wagging motion provide important state-of-the-art challenges for benchmarking high quality potential energy surfaces as well as furthering the development of efficient computational methods for multidimensional QM dynamics calculations. It is our hope that such synergism between high-resolution spectroscopic efforts, ab initio chemistry, and rigorous dynamical theory will help elucidate the role of this important radical in diverse venues ranging from combustion chemistry to chemistry in the interstellar medium.

AUTHOR INFORMATION

Notes

The authors declare no competing financial interest.

ACKNOWLEDGMENTS

This work was supported by grants from the Department of Energy (DE-FG02-09ER16021), with initial funds for construction of the slit jet laser spectrometer provided by the National Science Foundation (CHE 1012685 and PHY 1125844).

REFERENCES

(1) Johnson, R. D.; Hudgens, J. W. Structural and Thermochemical Properties of Hydroxymethyl (CH_2OH) Radicals and Cations Derived from Observations of Electronic Spectra and from ab Initio Calculations. *J. Phys. Chem.* **1996**, *100*, 19874.

(2) Kamarchik, E.; Rodrigo, C.; Bowman, J. M.; Reisler, H.; Krylov, A. I. Overtone-Induced Dissociation and Isomerization Dynamics of the Hydroxymethyl Radical (CH_2OH and CD_2OH). I. A Theoretical Study. *J. Chem. Phys.* **2012**, *136*, 084304.

(3) Li, J.; Zhao, Z.; Kazakov, A.; Chaos, M.; Dryer, F. L.; Scire, J. J., Jr. A Comprehensive Kinetic Mechanism for CO, CH_2O, and CH_3OH combustion. *Int. J. Chem. Kinet.* **2006**, *39*, 109.

(4) Westbrook, C. K.; Dryer, F. L. A Comprehensive Mechanism for Methanol Oxidation. *Combust. Sci. Technol.* **1979**, *20*, 125.

(5) Jodkowski, J. T.; Rayez, M.-T.; Rayez, J.-C.; Berces, T.; Dobe, S. Theoretical Study of the Kinetics of the Hydrogen Abstraction from Methanol. 3. Reaction of Methanol with Hydrogen Atom, Methyl, and Hydroxyl Radicals. *J. Phys. Chem. A* **1999**, *103*, 3750.

(6) Ruscic, B.; Berkowitz, J. Heat of Formation of Hydroxymethyl and Methanol D0(H-CH_2OH). *J. Phys. Chem.* **1993**, *97*, 11451.

(7) Xu, S.; Lin, M. C. Theoretical Study on the Kinetics for OH Reactions with CH_3OH and C_2H_5OH. *Proc. Combust. Inst.* **2007**, *31*, 159.

(8) Taatjes, C. A.; Hansen, N.; Osborn, D. L.; Kohse-Hoinghaus, K.; Cool, T. A.; Westmoreland, P. R. "Imaging" Combustion Chemistry via Multiplexed Synchrotron-Photoionization Mass Spectrometry. *Phys. Chem. Chem. Phys.* **2008**, *10*, 20.

(9) Taatjes, C. A.; Osborn, D. L.; Selby, T. M.; Meloni, G.; Fan, H. Y.; Pratt, S. T. Absolute Photoionization Cross-Section of the Methyl Radical. *J. Phys. Chem. A* **2008**, *112*, 9336.

(10) Cool, T. A.; Nakajima, K.; Taatjes, C. A.; McIlroy, A.; Westmoreland, P. R.; Law, M. E.; Morel, A. Studies of a Fuel-Rich Propane Flame with Photoionization Mass Spectrometry. *Proc. Combust. Inst.* **2005**, *30*, 1681.

(11) Cool, T. A.; Wang, J.; Nakajima, K.; Taatjes, C. A.; McIlroy, A. Photoionization Cross Sections for Reaction Intermediates in Hydrocarbon Combustion. *Int. J. Mass. Spectrom.* **2005**, *247*, 18.

(12) Taatjes, C. A.; Hansen, N.; McIlroy, A.; Miller, J. A.; Senosiain, J. P.; Klippenstein, S. J.; Qi, F.; Sheng, L. S.; Zhang, Y. W.; Cool, T. A.; et al. Enols Are Common Intermediates in Hydrocarbon Oxidation. *Science* **2005**, *308*, 1887.

(13) Taatjes, C. A.; Klippenstein, S. J.; Hansen, N.; Miller, J. A.; Cool, T. A.; Wang, J.; Law, M. E.; Westmoreland, P. R. Synchrotron Photoionization Measurements of Combustion Intermediates: Photoionization Efficiency and Identification of C_3H_2 Isomers. *Phys. Chem. Chem. Phys.* **2005**, *7*, 806.

(14) Dobe, S.; Otting, M.; Temps, F.; Wagner, H. G.; Ziemer, H. Fast-Flow Kinetic Studies of the Reaction $CH_2OH + HCl \rightarrow CH_3OH + Cl$: The Heat of Formation of Hydroxymethyl. *Ber. Bunsenges. Phys. Chem. Chem. Phys.* **1993**, *97*, 877.

(15) Dobe, S.; Temps, F.; Wagner, H. G.; Ziemer, H.; Berces, T. Kinetics of the Reaction between Hydroxymethyl Radicals and Hydrogen Atoms. *J. Phys. Chem.* **1994**, *98*, 9792.

(16) Nesbitt, F. L.; Payne, W. A.; Stief, L. J. Kinetic Studies of the Reaction of the Hydroxymethyl Radical with Nitric Oxide and Nitrogen Dioxide. *J. Phys. Chem.* **1989**, *93*, 5158.

(17) Heicklen, J. *Atmospheric Chemistry*; Academic Press: New York, 1976.

(18) Seinfeld, J. H.; Pandis, S. N. *Atmospheric Chemistry and Physics: From Air Pollution to Climate Change*, 2nd ed.; John Wiley & Sons: New York, 2006.

(19) Niki, H.; Maker, P. D.; Savage, C. M.; Breitenbach, L. P. Mechanism for Hydroxyl Radical Initiated Oxidation of Olefin−Nitric Oxide Mixtures in Parts Per Million Concentrations. *J. Phys. Chem.* **1978**, *82*, 135.
(20) Atkinson, R.; Arey, J. Gas-Phase Tropospheric Chemistry of Biogenic Volatile Organic Compounds: A Review. *Atmos. Environ.* **2003**, *37*, S197.
(21) Bennett, C. J.; Chen, S. H.; Sun, B. J.; Chang, A. H. H.; Kaiser, R. I. Mechanistical Studies on the Irradiation of Methanol in Extraterrestrial Ices. *Astrophys. J.* **2007**, *660*, 1588.
(22) Bennett, C. J.; Kaiser, R. I. On the Formation of Glycolaldehyde ($HCOCH_2OH$) and Methyl Formate ($HCOOCH_3$) in Interstellar Ice Analogs. *Astrophys. J.* **2007**, *661*, 899.
(23) Garrod, R. T.; Weaver, S. L. W.; Herbst, E. Complex Chemistry in Star-Forming Regions: An Expanded Gas-Grain Warm-up Chemical Nodel. *Astrophys. J.* **2008**, *682*, 283.
(24) Laas, J. C.; Garrod, R. T.; Herbst, E.; Weaver, S. L. W. Contributions from Grain Surface and Gas Phase Chemistry to the Formation of Methyl Formate and its Structural Isomers. *Astrophys. J.* **2011**, *728*, 71.
(25) Fortman, S. M.; Medvedev, I. R.; Neese, C. F.; De Lucia, F. C. How Complete Are Astrophysical Catalogs for the Millimeter and Submillimeter Spectral Region? *Astrophys. J. Lett.* **2010**, *725*, L11.
(26) Lees, R. M.; Xu, L. H.; Billinghurst, B. E.; Appadoo, D. R. T. Weeding the Cosmos: FIR Synchrotron Spectroscopy of Methanol at the Canadian Light Source. *J. Mol. Struct.* **2011**, *993*, 269.
(27) Pearson, J. C.; Drouin, B. J.; Yu, S. S.; Gupta, H. Microwave Spectroscopy of Methanol between 2.48 and 2.77 THz. *J. Opt. Soc. Am. B* **2011**, *28*, 2549.
(28) Pearson, J. C.; Brauer, C. S.; Drouin, B. J.; Xu, L. H. The Rotational Spectrum of Methanol in the Third Excited Torsional State. *Can. J. Phys.* **2009**, *87*, 449.
(29) Xu, L. H.; Fisher, J.; Lees, R. M.; Shi, H. Y.; Hougen, J. T.; Pearson, J. C.; Drouin, B. J.; Blake, G. A.; Braakman, R. Torsion-Rotation Global Analysis of the First Three Torsional States (nu(t)=0, 1, 2) and Terahertz Database for Methanol. *J. Mol. Spectrosc.* **2008**, *251*, 305.
(30) Bowman, J. M.; Carrington, T.; Meyer, H. D. Variational Quantum Approaches for Computing Vibrational Energies of Polyatomic Molecules. *Mol. Phys.* **2008**, *106*, 2145.
(31) Bowman, J. M.; Huang, X. C.; Handy, N. C.; Carter, S. Vibrational Levels of Methanol Calculated by the Reaction Path Version of MULTIMODE, Using an ab Initio, Full-Dimensional Potential. *J. Phys. Chem. A* **2007**, *111*, 7317.
(32) Pagsberg, P.; Munk, J.; Sillesen, A.; Anastasi, C. UV Spectrum and Kinetics of Hydroxymethyl Radicals. *Chem. Phys. Lett.* **1988**, *146*, 375.
(33) Radford, H. E.; Evenson, K. M.; Jennings, D. A.; Far-infrared, L. M. R. Detection of Hydroxymethyl Radical. *Chem. Phys. Lett.* **1981**, *78*, 589.
(34) Harwit, M. The Herschel Mission. In *Astronomy at IR/Submm and the Microwave Backgound*; Wesselius, P. R., Olthof, H., Eds.; Pergamon-Elsevier Science Ltd: Kidlington, U.K., 2004; Vol. *34*, p 568.
(35) Magnelli, B.; Lutz, D.; Santini, P.; Saintonge, A.; Berta, S.; Albrecht, M.; Altieri, B.; Andreani, P.; Aussel, H.; Bertoldi, F.; et al. A Herschel View of the Far-infrared Properties of Submillimetre Galaxies. *Astron. Astrophys.* **2012**, *539*, A155.
(36) Pilbratt, G. L.; Riedinger, J. R.; Passvogel, T.; Crone, G.; Doyle, D.; Gageur, U.; Heras, A. M.; Jewell, C.; Metcalfe, L.; Ott, S.; et al. Herschel Space Observatory: An ESA Facility for Far-Infrared and Submillimetre Astronomy. *Astron. Astrophys.* **2010**, *518*, L1.
(37) Chen, F. W.; Davidson, E. R. Theoretical Study of the Electronic Spectrum and ESR of the CH_2OH Radical. *J. Phys. Chem. A* **2001**, *105*, 4558.
(38) Dixon, W. T.; Norman, R. O. C. Electron Spin Resonance Studies of Oxidation. 1. Alcohols. *J. Chem. Soc.* **1963**, 3119.
(39) Livingston, R.; Zeldes, H. Paramagnetic Resonance Study of Liquids During Photolysis: Hydrogen Peroxide and Alcohols. *J. Chem. Phys.* **1966**, *44*, 1245.
(40) Hudson, A. Alternating Line Widths in the Electron Spin Resonance Spectrum of Hydroxymethyl Radical. *J. Chem. Soc. A* **1969**, 2513.
(41) Hudson, A.; Luckhurst, G. R. Electron Resonance Line Shapes of Radicals in Solution. *Chem. Rev.* **1969**, *69*, 191.
(42) Jacox, M. E.; Milligan, D. E. Matrix Isolation Study of the Vacuum-Ultraviolet Photolysis of Methanol: The Infrared Spectrum of the CH_2OH Free Radical. *J. Mol. Spectrosc.* **1973**, *47*, 148.
(43) Jacox, M. E. The Reaction of Excited Argon Atoms and of F Atoms with Methanol. Vibrational Spectrum of CH_2OH Isolated in Solid Argon. *Chem. Phys.* **1981**, *59*, 213.
(44) Bernardi, F.; Epiotis, N. D.; Cherry, W.; Schlegel, H. B.; Whangbo, M.-H.; Wolfe, S. A Molecular Orbital Interpretation of the Static, Dynamic, and Chemical Properties of CH_2X Radicals. *J. Am. Chem. Soc.* **1976**, *98*, 469.
(45) Ha, T.-K. A Theoretical Study of the Internal Rotation and Inversion in Hydroxymethyl Radical (CH_2OH). *Chem. Phys. Lett.* **1975**, *30*, 379.
(46) Radford, H. E. The Fast Reaction of CH_2OH with O_2. *Chem. Phys. Lett.* **1980**, *71*, 195.
(47) Dulcey, C. S.; Hudgens, J. W. Detection of Hydroxymethyl (CH_2OH) Radicals by Resonance-Enhanced Multiphoton Ionization Spectroscopy. *J. Phys. Chem.* **1983**, *87*, 2296.
(48) Dulcey, C. S.; Hudgens, J. W. Multiphoton Ionization Spectroscopy of the Hydroxymethyl Radical. *Bull. Soc. Chim. Belg.* **1983**, *92*, 583.
(49) Dulcey, C. S.; Hudgens, J. W. Multiphoton Ionization Spectroscopy and Vibrational Analysis of a 3p Rydberg State of the Hydroxymethyl Radical. *J. Chem. Phys.* **1986**, *84*, 5262.
(50) Aristov, V.; Conroy, D.; Reisler, H. Symmetry and Lifetime of the Hydroxymethyl Radical in the 3p Rydberg State. *Chem. Phys. Lett.* **2000**, *318*, 393.
(51) Feng, L.; Demyanenko, A. V.; Reisler, H. O−D Bond Dissociation from the 3s State of Deuterated Hydroxymethyl Radical (CH_2OD). *J. Chem. Phys.* **2003**, *118*, 9623.
(52) Feng, L.; Demyanenko, A. V.; Reisler, H. Competitive C−H and O−D Bond Fission Channels in the UV Photodissociation of the Deuterated Hydroxymethyl Radical CH_2OD. *J. Chem. Phys.* **2004**, *120*, 6524.
(53) Feng, L.; Huang, X.; Reisler, H. Photodissociative Spectroscopy of the Hydroxymethyl Radical (CH_2OH) in the 3s and 3px States. *J. Chem. Phys.* **2002**, *117*, 4820.
(54) Feng, L.; Reisler, H. Photodissociation of the Hydroxymethyl Radical from the (3pz) State: H_2CO and HCOH Products. *J. Phys. Chem. A* **2004**, *108*, 9847.
(55) Feng, L.; Wei, J.; Reisler, H. Rotationally Resolved Infrared Spectroscopy of the Hydroxymethyl Radical (CH_2OH). *J. Phys. Chem. A* **2004**, *108*, 7903.
(56) Wei, J.; Karpichev, B.; Reisler, H. Unimolecular Processes in CH_2OH below the Dissociation Barrier: O···H Stretch Overtone Excitation and Dissociation. *J. Chem. Phys.* **2006**, *125*, 034303.
(57) Werner, H.-J.; Knowles, P. J.; Lindh, R.; Schutz, M.; Celani, P.; Korona, T.; Manby, F. R.; Rauhut, G.; Amos, R. D.; Bernhardsson, A.; et al. *MOLPRO*, version 2002.6; Cardiff University: Cardiff, U.K., 2003.
(58) Davis, S.; Farnik, M.; Uy, D.; Nesbitt, D. Concentration Modulation Spectroscopy with a Pulsed Slit Supersonic Discharge Expansion Source. *Chem. Phys. Lett.* **2001**, *344*, 23.
(59) Davis, S.; Uy, D.; Nesbitt, D. J. Laser Spectroscopy of Jet-Cooled Ethyl Radical: Infrared Studies in the CH_2 Stretch Manifold. *J. Chem. Phys.* **2000**, *112*, 1823.
(60) Dong, F.; Davis, S.; Nesbitt, D. Slit Discharge IR Spectroscopy of a Jet-Cooled Cyclopropyl Radical: Structure and Intramolecular Tunneling Dynamics. *J. Phys. Chem. A* **2006**, *110*, 3059.
(61) Pine, A. S. High-Resolution Methane ν_3-Band Spectra Using a Stabilized Tunable Difference-Frequency Laser System. *J. Opt. Soc. Am.* **1976**, *66*, 97.

(62) Ahmed, M.; Peterka, D. S.; Suits, A. G. Imaging H Abstraction Dynamics in Crossed Molecular Beams: Cl + ROH Reactions. *Phys. Chem. Chem. Phys.* **2000**, *2*, 861.
(63) Dobe, S.; Berces, T.; Turanyi, T.; Marta, F.; Grussdorf, J.; Temps, F.; Wagner, H. G. Direct Kinetic Studies of the Reactions Br + CH_3OH and CH_2OH + HBr: The Heat of Formation of CH_2OH. *J. Phys. Chem.* **1996**, *100*, 19864.
(64) Smith, J. D.; Desain, J. D.; Taatjes, C. A. Infrared Laser Absorption Measurements of HCl(v = 1) Production in Reactions of Cl Atoms with Isobutane, Methanol, Acetaldehyde and Toluene at 295 K. *Chem. Phys. Lett.* **2002**, *366*, 417.
(65) Bunker, P. R.; Jensen, P. *Molecular Symmetry and Spectroscopy*; NRC Research Press: Ottawa, Canada, 1998.
(66) Bowman, J. M.; Carter, S.; Huang, X. C. MULTIMODE: A Code to Calculate Rovibrational Energies of Polyatomic Molecules. *Int. Rev. Phys. Chem.* **2003**, *22*, 533.
(67) Braams, B. J.; Bowman, J. M. Permutationally Invariant Potential Energy Surfaces in High Dimensionality. *Int. Rev. Phys. Chem.* **2009**, *28*, 577.
(68) Bowman, J. M.; Huang, X. C.; Carter, S. Full Dimensional Calculations of Vibrational Energies of H_3O^+ and D_3O. *Spectrochim. Acta* **2002**, *58*, 839.
(69) Sharma, A. R.; Bowman, J. M.; Nesbitt, D. J. Large-Amplitude Dynamics in Vinyl Radical: The Role of Quantum Tunneling As an Isomerization Mechanism. *J. Chem. Phys.* **2012**, *136*, 034305.
(70) Sharma, A. R.; Wu, J. Y.; Braams, B. J.; Carter, S.; Schneider, R.; Shepler, B.; Bowman, J. M. Potential energy surface and MULTI-MODE vibrational analysis of $C_2H_3^+$. *J. Chem. Phys.* **2006**, *125*, 224306.
(71) Townsend, D.; Lahankar, S. A.; Lee, S. K.; Chambreau, S. D.; Suits, A. G.; Zhang, X.; Rheinecker, J.; Harding, L. B.; Bowman, J. M. The Roaming Atom: Straying from the Reaction Path in Formaldehyde Decomposition. *Science* **2004**, *306*, 1158.
(72) Frisch, M. J.; Trucks, G. W.; Schlegel, H. B.; Scuseria, G. E.; Robb, M. A.; Cheeseman, J. R.; Zakrzewski, V. G.; Montgomery, J. A., Jr.; Stratmann, R. E.; Burant, J. C.; et al.. *Gaussian 98*, revision A.7; Gaussian, Inc.: Pittsburgh, PA, 1998.